British Journal of Pharmacology (1998) 124, 729–741
http://www.stockton-press.co.uk/bjp

Pharmacological analysis of the activity of the adenosine uptake inhibitor, dipyridamole, on the sinoatrial and atrioventricular nodes of the guinea-pig

B.J. Meester, [2]N.P. Shankley, N.J. Welsh, [1]F.L. Meijler & J.W. Black

Analytical Pharmacology, Rayne Institute, King's College School of Medicine & Dentistry, 123, Coldharbour Lane, London SE5 9NU, U.K. and [1]Interuniversity Cardiology Institute of the Netherlands, Catharijnesingel 52, 3511 GC Utrecht, The Netherlands

1 Dipyridamole potentiates the effects of adenosine on the heart by inhibiting adenosine uptake. The effects of dipyridamole on both adenosine and N-ethylcarboxamidoadenosine (NECA) concentration-effect (E/[A]) curves were compared on the AV node, in guinea-pig isolated perfused hearts, and on the SA node, in isolated right atria, by measuring dromotropic and chronotropic responses, respectively. In the absence of dipyridamole, adenosine was significantly more potent on the AV node than SA node (AV $p[A]_{50} = 4.95 \pm 0.10$, SA $p[A]_{50} = 3.62 \pm 0.10$). In contrast, NECA and adenosine in the presence of dipyridamole were approximately equiactive in the two assays (NECA: AV $p[A]_{50} = 7.07 \pm 0.07$; SA $p[A]_{50} = 7.30 \pm 0.08$; adenosine: AV $p[A]_{50} = 6.49 \pm 0.08$; SA $p[A]_{50} = 6.27 \pm 0.05$). Dipyridamole was significantly more potent in enhancing the effects of adenosine on the SA node than on the AV node (pK_i values estimated by Kenakin's method (1981): AV node $= 8.18 \pm 0.14$; SA node $= 8.75 \pm 0.08$).

2 The difference in pK_i values did not appear to be due to dipyridamole expressing other actions because concentrations of dipyridamole which saturated the adenosine transporter had no effect on the NECA E/[A] curves in either assay. However, the test of another assumption of Kenakin's method, that adenosine taken up into cells is pharmacologically inactive, failed on the AV node assay because a significant potentiating interaction was found between adenosine and NECA. The interaction was concentration-dependent, reciprocal to the extent that pre-incubation with either agonist potentiated the other and was concluded to be due to an intracellular action of adenosine as the potentiation disappeared in the presence of dipyridamole.

3 An explanatory model was developed to account for the data obtained using existing pharmacological concepts of ligand action in isolated tissue bioassays. In the model, adenosine, but not NECA, was assumed to be subject to saturable agonist uptake, an uptake which was competitively blocked by dipyridamole. Adenosine and NECA were assumed to act extracellularly at adenosine A_1-receptors. In the AV node, but not the SA node, the adenosine transported into the cells was assumed to potentiate the effects of adenosine A_1-receptor activation. For the AV node assay, the model predicted that potentiation of adenosine by uptake blockade is offset by a simultaneous decrease in potentiation due to the intracellular action of adenosine. All of the experimental data obtained in the study could be accounted for by the model including the apparent differences in potency of adenosine in the absence of dipyridamole and the pK_i values for dipyridamole.

Keywords: Atrioventricular node; sinoatrial node; adenosine receptor; adenosine uptake

Introduction

Physiologically, the exercise-related increase in heart rate is associated with a shortening of the PR-interval of the electrocardiogram. Exercise-related shortening is mainly due to a decrease in the conduction time in the atrioventricular (AV) node caused by enhanced activity in the sympathetic nerves. This effect can be annulled by blockade of β-adrenoceptors. Paradoxically, however, AV nodal transmission progressively slows, to end in heart block, when atrial frequency is increased by electrical stimulation. This phenomenon is an intrinsic property of the AV node and thus is not due to the conduction-delaying effects of the parasympathetic nerve supply.

A characteristic action of adenosine and the adenine nucleotides is concentration-dependent slowing of AV nodal transmission (Drury & Szent-Gyorgi, 1929). Recently, further interest in the physiological role of adenosine in AV nodal function was generated when Jenkins and Belardinelli (1988) investigated the role of adenosine on AV nodal transmission in guinea-pig isolated, perfused hearts. They found that the adenosine receptor antagonist, BW-A1433, increased the maximal AV conduction time that did not result in second or third degree AV block. They also found that blocking the uptake of adenosine by dipyridamole augmented the frequency-dependent conduction delay, most notably at the higher frequencies. This dipyridamole-induced effect was blocked by BW-A1433 (a selective A_1-receptor antagonist). Jenkins & Belardinelli (1988) concluded that the release of adenosine appeared to increase under conditions of increased metabolic demand and postulated that it functions as a negative feedback signal to protect the ventricles from excessive work by causing AV block. Although these results suggest that adenosine is mainly a cardioprotective agent, it is still not clear whether adenosine, in some way, may contribute to the frequency-dependent delay in the AV node.

We have revisited this problem in the light of continuing uncertainties about the classification of adenosine sites of action in the heart. Is the adenosine receptor a 'classical' A_1-receptor or perhaps a subtype (Ribeiro & Sebastiao, 1986)? Does adenosine have a physiologically-relevant intracellular

[2] Author for correspondence.

site of action, such as the so-called P-site (Londos & Wolff, 1977)? If so, could this putative intracellular action of adenosine be exposed by blocking the uptake of adenosine by dipyridamole? Initially, these questions were addressed by comparing the effect of dipyridamole on the chronotropic and dromotropic responses to adenosine on sinoatrial (SA) and AV nodes of the guinea-pig heart. Here, we present the results of the analysis and the development of an explanatory model to account for the data obtained. Preliminary accounts of the study have been presented to the British Pharmacological Society (Meester *et al*., 1993; 1994a,b).

Methods

Guinea-pig isolated right atrium (SA node) preparation

Chronotropic responses were measured in isolated, spontaneously-beating, right atria from male guinea-pigs (Dunkin-Hartley, 300–400 g), prepared according to previously described methods (Black *et al*., 1985). In brief, the atria were suspended in 20 ml of Krebs-Henseleit (K-H) solution (composition, mM: Na^+ 143, K^+ 5.9, Ca^{2+} 2.5, Mg^{2+} 1.2, Cl^- 128, $H_2PO_4^-$ 2.2, HCO_3^- 24.9, SO_4^{2-} 1.2 and dextrose 10) maintained at 37 ± 0.3°C and gassed with 95% O_2 and 5% CO_2. Tissues were loaded with an initial 0.5 g resting tension. Each isometric transducer output was amplified (Ormed 3559) and processed by a digital rate meter (Ormed 4461) which gave a direct readout of rate (beats min^{-1}) continuously displayed on a potentiometric chart recorder.

Guinea-pig isolated perfused heart (AV node) preparation

Dromotropic effects were measured in isolated hearts of male guinea-pigs (Dunkin-Hartley, 200–300 g). The hearts were retrogradely perfused via the aorta (Langendorff preparation) at a constant perfusion pressure of 74 cmH_2O (Döhring & Dehnert, 1986) with K-H solution, maintained at 35 ± 0.3°C and gassed with 95% O_2 : 5% CO_2. The preparations were allowed to stabilize for 20–25 min. The sinoatrial region and most of the right atrium were excised. Removal of the SA node allowed the heart to be driven at a constant, high, rate of atrial pacing (3.5 Hz). Hearts were electrically stimulated (Grass S88) with square wave pulses (1 ms duration, twice threshold voltage) delivered via a stimulus-isolation unit (Grass SIU5) using a bipolar silver electrode placed on the left atrium. Removal of most of the right atrium allowed for the placement of two teflon-coated electrodes (Ag-5T), one on the intra-atrial septum and one on the left ventricle. The extracellular bipolar electrogram (EG) was then displayed on a digital oscilloscope (Nicolet 4094) at a sweep speed of 1 ms or 500 ms per point. The stimulus-to-R wave (SR) interval, calculated from the EG using Nicolet data analysis software (Mathpak 4094), was used as a measure of AV conduction (ms).

The temperature was reduced from 37 to 35°C as this was found to abolish the spontaneous rhythms which occasionally arose at frequencies above the rate of external pacing. This step was taken in preference to increasing the rate of pacing which would have had the effect of reducing the experimental window in which agonist effects could be measured.

Experimental protocols

Guinea-pig isolated right atrium assay Six isolated right atrium preparations were used simultaneously and were allocated to control and treatment groups so that, as far as was practical, the design was balanced over organ baths and days. Control preparations were dosed with the maximal amount of vehicle used for any one treatment. None of the vehicles (see Compounds) had a significant effect on basal rate. Preparations were allowed to stabilize for 60 min during which time the organ bath fluid was replaced with pre-warmed K-H solution at 15 min intervals. Adenosine receptor activation slows the pacemaker frequency. Therefore, to increase the size of the agonist 'window', histamine (3 μM, corresponding to $\sim$90% of the histamine maximum response) was added to the organ baths to increase basal rate from $\sim$200 to $\sim$300 beats min^{-1}. Timolol (3 μM, $\sim$3000-fold K_B at β_1-adrenoceptors, Blum-Kaelin *et al*., 1991) was added to annul possible β-adrenoceptor stimulation. Single agonist concentration-effect (E/[A]) curves were obtained by cumulative dosing at half-log unit concentration increments. The total amount of vehicle added to the organ baths during an experiment did not exceed 7% of the original bath volume.

Guinea-pig isolated perfused heart assay Two isolated perfused heart preparations were used simultaneously and treatments, including vehicle controls, were allocated across the three replicate experiments performed daily so that, as far as was practical, the design was balanced over organ baths and days. None of the vehicle controls had a significant effect on the basal SR-interval. The adenosine uptake blocker, dipyridamole, was added to the K-H reservoir and perfused for 25 min before single E/[A] curves were obtained. Both adenosine and NECA (5′-N-ethylcarboxamidoadenosine) were used as agonists; NECA has been shown not to be a substrate for the adenosine transporter (Clanachan *et al*., 1987). The agonists were administered into the perfusion lines at a fixed flow rate via a syringe pump. Preliminary experiments had shown that, at all concentrations of agonist, steady-state responses were always attained within 3 min for adenosine and 5 min for N-ethylcarboxamidoadenosine (NECA). The responses were measured from EG records displayed on an oscilloscope rather than from continuous chart records. Therefore, on the basis of the preliminary experiments, the responses to individual applications of agonist were recorded when a further 30 s had elapsed after the exposure times given above for each agonist.

Data analysis

Agonist concentration-effect curves Responses from the right atrium assays and isolated perfused hearts were expressed as changes in rate (Δ basal rate: beats min^{-1}) and SR-interval (Δ SR-interval: ms). The E/log[A] curves obtained in the right atria and isolated hearts had a parabolic rather than a classical sigmoidal shape. Presumably, this was because the maximal responses were limited by either an abrupt onset of SA or AV block. Accordingly, in the right atrium assay the response to the highest concentration of agonist that produced a stable rate change and, in the isolated heart assay, the value of the longest stable SR-interval immediately before block, was taken as the maximum response (α). The concentration of agonist required to produce 50% of this maximal inhibitory action ($[A]_{50}$) was estimated graphically for each individual curve. On the assumption that these values are log-normally distributed, $\log[A]_{50}$ values were used for subsequent analysis. Dosing was stopped in all preparations when SA or AV node block was achieved. In practice, the agonist concentration which produced the highest response before the onset of SA or AV block varied between the individual preparations. Thus, strictly, meaningful average ($\pm$s.e.mean) data values could only be calculated at agonist concentrations which produced

responses in all preparations. In an attempt to illustrate more of the data, the mean value of the highest response obtained in each preparation, regardless of the concentration of agonist, was calculated and expressed as a function of the average log[A] which produced these responses.

Estimation of the pK_i for dipyridamole

Estimates of the equilibrium dissociation constants for dipyridamole were made using the method described by Kenakin (1981). The method is based on Waud's (1969) model which describes the effect of a saturable uptake process on agonist concentration in the receptor compartment. The model assumes that the rate of entry of the agonist is governed and limited by bulk diffusion and that the removal process follows Michaelis-Menten kinetics. Kenakin (1981) further developed the model to allow estimation of the leftward shift of the substrate agonist concentration-effect curve in the presence of increasing concentrations of a competitive uptake inhibitor. The method assumes that the agonist concentration in the receptor compartment is negligible compared to the equilibrium dissociation constant for the agonist at the uptake site so that the system operates under pseudo-first order conditions. The following equation describes the effect of an uptake inhibitor, I, in terms of its equilibrium dissociation constant for the uptake process (K_i) and the degree of potentiation of agonist, X, expressed as the ratio of equi-effective agonist concentrations in the absence and presence of the uptake inhibitor. X_{max} is the maximum degree of potentiation achieved when the uptake process is completely inhibited:

$$\log\frac{X_{max}(X-1)}{(X_{max}-X)} = \log[I] - \log K_i \qquad (1)$$

By analogy with the Schild plot, a plot of log $\{X_{max}(X-1)/(X_{max}-X)\}$ as a function of log [I] should yield a straight line with unit slope and the x-intercept is equal to the pK_i value. Data were fitted to this function by standard linear regression.

All data are presented as mean ± s.e.mean. Differences between sets of curve parameters (α and $\log[A]_{50}$) obtained within an experiment were tested by one-way analysis of variance. Differences in $\log[A]_{50}$ estimates made in different experiments and assays were compared by *t* test. The reliability of this type of comparison between experimental systems is based on the assumption that there is no difference bias between the assays. Differences were considered significant when $P<0.05$.

Compounds

Adenosine, dipyridamole and NECA were purchased from Sigma Chemical Company Ltd. (U.K.). Adenosine and dipyridamole were prepared as 20 mM stock solutions in distilled water. NECA was initially dissolved in 0.1 M HCl to 20 mM. Further serial dilutions of the stock solutions were made in distilled water.

Results

Are the effects of adenosine and NECA on the SA and AV nodal assays comparable?

Adenosine produced a concentration-dependent inhibition of both SA and AV nodal activity which terminated abruptly in SA pacemaker arrest or AV conduction block. The log concentration-effect curves were convex to the x-axis with no upper asymptote as though they were the lower regions of a sigmoid function (Figure 1). The shape of NECA curves were indistinguishable from those of adenosine. Locating such curves by the concentration needed for half-maximal effect, $[A]_{50}$, does not have the same meaning as an $[A]_{50}$ calculated for a full sigmoid function. However, as the concentration-effect curves on the two tissues appeared to have a similar shape, a null-method comparison of $[A]_{50}$ values seemed allowable. Adenosine in the AV node ($p[A]_{50} = 4.95 \pm 0.10$) was significantly more potent than in the SA node ($p[A]_{50} = 3.62 \pm 0.10$). In contrast, NECA was approximately equiactive in both assays (Figure 1; SA node, $p[A]_{50} = 7.30 \pm 0.08$; AV node, $p[A]_{50} = 7.07 \pm 0.07$) suggesting that the adenosine potency differences were not somehow due to an invalid comparison of assays.

Does dipyridamole have effects on basal activity in the SA and AV node assays?

Jenkins & Belardinelli (1988) reported that, under conditions of excessive stimulation, adenosine is released in cardiac preparations. However, under the low frequency assay conditions used here, effects of the adenosine transport inhibitor were not expected on basal activity.

At low concentrations (0.1 to 1 μM), dipyridamole had no effect on the basal conductance in the AV node assay (Figure 2c). However, at higher concentrations (3 and 10 μM) there was an apparent concentration-dependent increase in SR interval and at 30 μM (data not shown) there was a large increase in basal SR-interval which, within minutes of starting the infusion of adenosine, in 3 out of 4 hearts, progressed to AV-block. A similar concentration-dependent effect was obtained on basal rate in the SA node assay. Although, strictly, not significant as tested, presumably due to the large variances, the decrease in basal rate obtained with the highest concentration of dipyridamole (30 μM) was 57 ± 21 beats min^{-1} ($P = 0.06$) which was equivalent to ~30% of the maximum response subsequently obtained by addition of adenosine.

Is dipyridamole equi-effective in the SA and AV node assays?

Dipyridamole produced a significant concentration-dependent leftward shift of adenosine concentration-effect curves in both assays (Figure 2). The log ratio of the $[A]_{50}$ values, calculated at the minimum concentrations of dipyridamole apparently necessary to saturate the uptake (1 μM in SA node and 3 μM in

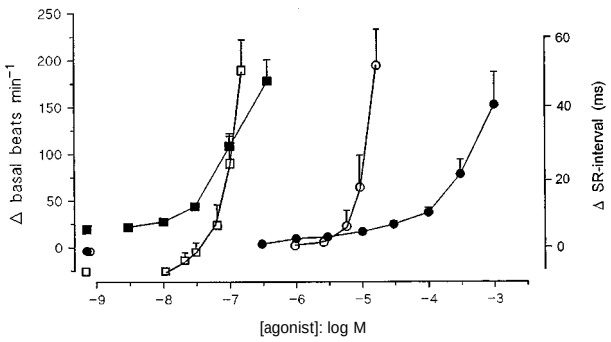

Figure 1 Adenosine (circles) and NECA (squares) concentration-effect curve data obtained in the SA (solid symbols, Δ basal beats min^{-1}) and AV (open symbols, Δ SR-interval) node assays. Values represent mean of 5/7 preparations (see Table 1 for details); vertical lines show s.e.mean.

AV node), was 2.65±0.11 in the SA node and 1.54±0.11 in AV node so that the $p[A]_{50}$ values for adenosine in the presence of dipyridamole were now not significantly different between the assays. This difference in the maximum degree of potentiation (X_{max}, Equation (1)) achieved by blocking the transporter was accompanied by a significant difference in the apparent affinity of dipyridamole as estimated by applying Kenakin's (1981) method (Equation 1) to the data obtained in the absence and presence of dipyridamole (AV node: $pK_i = 8.18 \pm 0.14$, slope = 0.88±0.14; SA node $pK_i = 8.75 \pm 0.08$, slope = 1.13±0.24).

The different apparent pK_i values for dipyridamole could be regarded as preliminary evidence for different adenosine transporters in the AV and SA nodes.

Does dipyridamole affect NECA E/[A] curves?

One assumption underlying Kenakin's method is that dipyridamole does not express an additional, tissue-dependent, action which could affect its apparent affinity for the transporter system. This was investigated by testing the effect of dipyridamole on NECA E/[A] curves.

Dipyridamole, at a concentration which appeared to saturate the transport of adenosine (1 μM in SA node, 3 μM in AV node) had no effect on the NECA concentration-effect curve in either assay as judged by comparison of $log[A]_{50}$ values (Figure 3a, log dose-ratios; AV node = 0.05±0.08, SA node = 0.04±0.11). Therefore, the effects of dipyridamole on adenosine could be assumed to depend solely on its transporter blocking action.

Is the adenosine transported into cells pharmacologically inactive?

Another assumption underlying Kenakin's method is that the transported adenosine is pharmacologically inactive so that the action of dipyridamole is solely due to prevention of the loss of adenosine from the receptor compartment. If adenosine was

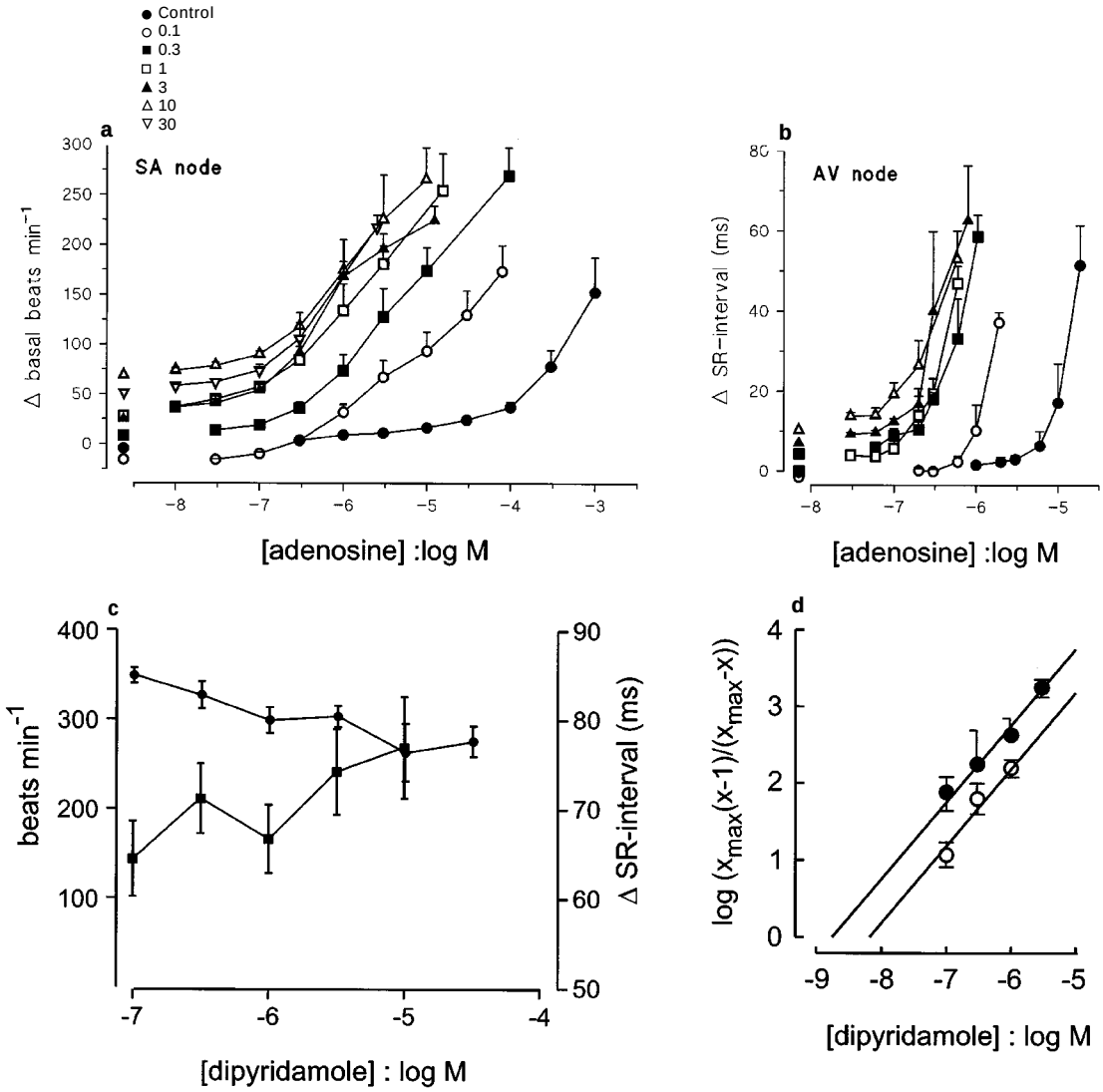

Figure 2 Adenosine concentration-effect curve data obtained in the (a) SA node and (b) AV node assays in the absence (control) and presence of 0.1, 0.3, 1, 3, 10 and 30 μM dipyridamole. Values represent mean and vertical lines s.e.mean of 5/7 preparations. (c) The effect of dipyridamole on basal rate (circles, beats min^{-1}) in the SA node and basal conductance (squares, ms) in the AV node obtained in the same experiments (SA node control group basal rate = 332.6±12.9, AV node control group basal conductance = 65.8±2.9 ms). (d) The relationship between the concentration of dipyridamole and the degree of potentiation, expressed according to equation (1) in the methods, in the SA (solid circles) and AV node (open circles), respectively. The solid line represents the best fit obtained when the slope was constrained to unity, under which condition, apparent pK_i values for dipyridamole of 8.75±0.08 and 8.18±0.14 were estimated in the SA and AV node, respectively.

expressing intracellular actions then they could be exposed by an interaction between adenosine and NECA. If there was no interaction then the effects of the two agonists acting at a common receptor would be less than additive.

When the NECA concentration-effect curve in the SA node was repeated in the presence of 60 μM adenosine, a concentration calculated to produce about 20% of the maximum effect when given on its own, no significant differences were found (log dose-ratio = 0.04 ± 0.15) with respect to the control curve (Figure 4a). On the other hand, when an equivalent concentration of adenosine (10 μM) was used in the AV node, the subsequent NECA concentration-

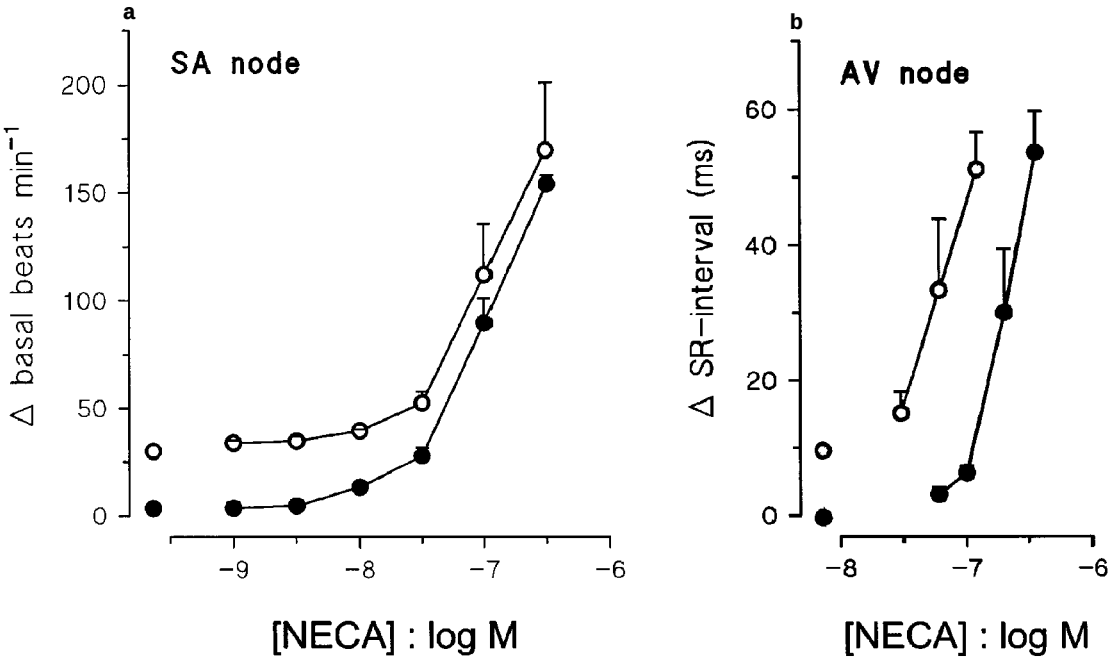

Figure 3 NECA concentration-effect curve data obtained in the (a) SA and (b) AV node assays in the absence (solid circles) and presence (open circles) of dipyridamole (1 μM SA node and 3 μM AV node). Values represent mean of 5/7 preparations; vertical lines show s.e.mean.

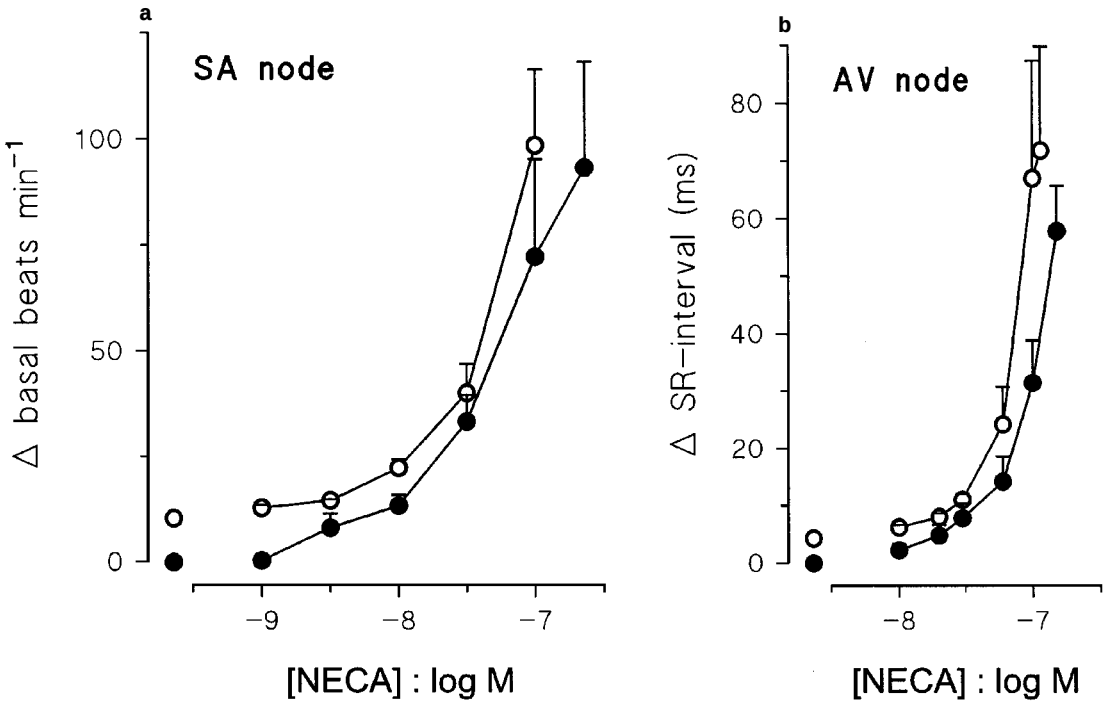

Figure 4 NECA concentration-effect curve data obtained in the (a) SA and (b) AV node assays in the absence (solid circles) and presence (open circles) of adenosine (60 μM in the SA node and 10 μM in the AV node). Values represent mean of 5 preparations; vertical lines show s.e.mean.

effect curve was significantly displaced to the left (log dose-ratio = 0.47 ± 0.10, Figure 4b).

This result indicated that adenosine was expressing an additional action in the AV node and posed three further questions which were addressed experimentally. Is the NECA-adenosine interaction dependent on the cellular uptake of adenosine? Is the effect of adenosine on the AV node concentration-dependent? Is the interaction reciprocal?

Is the NECA-adenosine interaction dependent on the cellular uptake of adenosine?

Dipyridamole was used to try to answer this question. The effects of dipyridamole on the control and potentiated curves are shown in Figure 6a and b and in Table 1. Dipyridamole displaced the adenosine control curve significantly to the left (log dose-ratio = 1.68 ± 0.11). However, in the presence of dipyridamole, the further addition of NECA did not now shift the adenosine curve (log dose-ratio = 1.37 ± 0.22 with respect to the control curve). On the other hand, dipyridamole, had no effect on the NECA curve as judged by location (log dose-ratio = 0.05 ± 0.08). In the presence of dipyridamole and adenosine, there was no longer a significant shift of the NECA curve (log dose-ratio = 0.25 ± 0.11). Therefore, abolishing the uptake of adenosine appears to block the potentiating interaction between adenosine and NECA.

Is the potentiation of NECA by adenosine concentration-dependent?

The control adenosine concentration-effect curve obtained in the first experiment (Figure 1a) was very steep; threshold responses occurred between 1 and 3 μM and heart block developed at concentrations greater than 15 μM. Therefore, adenosine concentrations of 6, 10 and 15 μM were chosen for examining the concentration-dependence of the adenosine-NECA interaction. The results are shown in Figure 5. In this experiment, the lowest concentration had no significant effect on the basal S-R interval but 10 and 15 μM increased the basal levels by 8.6 ± 3.0 and 4.0 ± 3.0 ms, respectively. In the presence of all three adenosine concentrations, the NECA concentration-effect curves were displaced significantly to the left. The log-dose ratio (that is, the ratios of $[A]_{50}$ values of adenosine-treated to control NECA curves) were 0.43 ± 0.14, 0.53 ± 0.13 and 1.31 ± 0.24 for adenosine concentrations of 6, 10 and 15 μM, respectively. Of particular interest is the observation that the sub-threshold concentration (6 μM) of adenosine nevertheless significantly potentiated the effects of NECA.

Is there a mutual potentiation between NECA and adenosine?

The answer to this question was sought as part of a larger randomized-block design experiment involving a control and four treatment groups for each agonist. All of the treatment groups and the results are set out in Table 1. For two of these treatment groups, NECA and adenosine concentration-effect curves were obtained in the presence of fixed concentrations of each other, to test for mutual potentiation, and also in the presence of fixed concentrations of themselves, to test for auto-potentiation. The results are shown graphically in Figure 6a and b. The NECA concentration-effect curve was significantly displaced to the left in the presence of 6 μM adenosine confirming the potentiating effect of adenosine (log dose-ratio = 0.55 ± 0.13). However, in the presence of 60 nM NECA

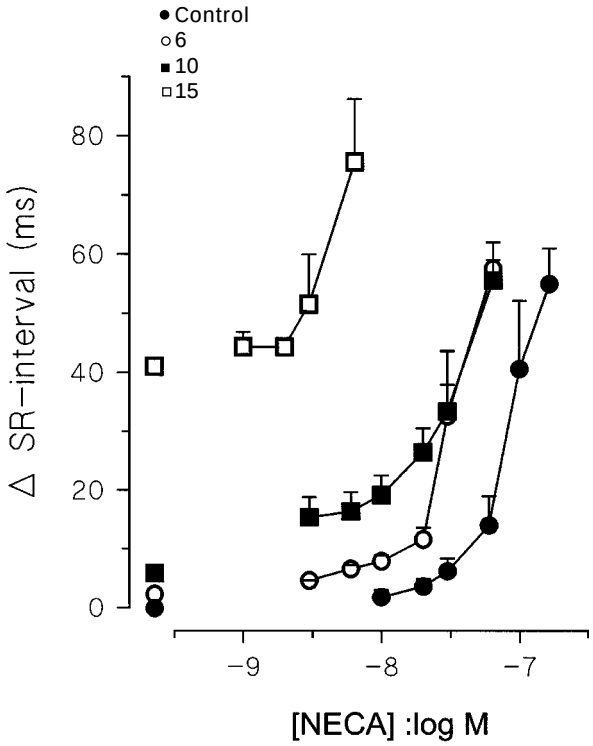

Figure 5 NECA concentration-effect curve data obtained in the AV node assay in the absence (control) and presence of 6, 10 and 15 μM adenosine. Values represent mean of 5/6 preparations; vertical lines show s.e.mean.

Table 1 Interaction between adenosine and NECA in the AV node assay

Agonist	*Treatment*	*Control p[A]$_{50}$*	*Treatment p[A]$_{50}$*	*Log p[A]$_{50}$ ratio*
	NECA 60 nM	4.76 ± 0.07	5.60 ± 0.19	0.84 ± 0.20*
	Dipyridamole 1 μM	4.76 ± 0.07	6.44 ± 0.09	1.68 ± 0.11*
Adenosine	Adenosine 6 μM	4.76 ± 0.07	5.10 ± 0.12	0.34 ± 0.14
	Dipyridamole 1 μM + NECA 60 nM	4.76 ± 0.07	6.13 ± 0.21	1.37 ± 0.22*
	Adenosine 6 μM	7.07 ± 0.07	7.62 ± 0.11	0.55 ± 0.13*
NECA	Dipyridamole 1 μM	7.07 ± 0.07	7.12 ± 0.04	0.05 ± 0.08
	NECA 60 nM	7.07 ± 0.07	7.14 ± 0.10	0.07 ± 0.12
	Dipyridamole + NECA 60 nM	7.07 ± 0.07	7.32 ± 0.09	0.25 ± 0.11

For definition of $[A]_{50}$ and details of data analysis see Methods. Values represent mean ± s.e.mean of 5/6 preparations. Statistical differences between values were assessed by one-way ANOVA combined with the Bonferroni method; *denotes a log dose-ratio significantly different from zero.

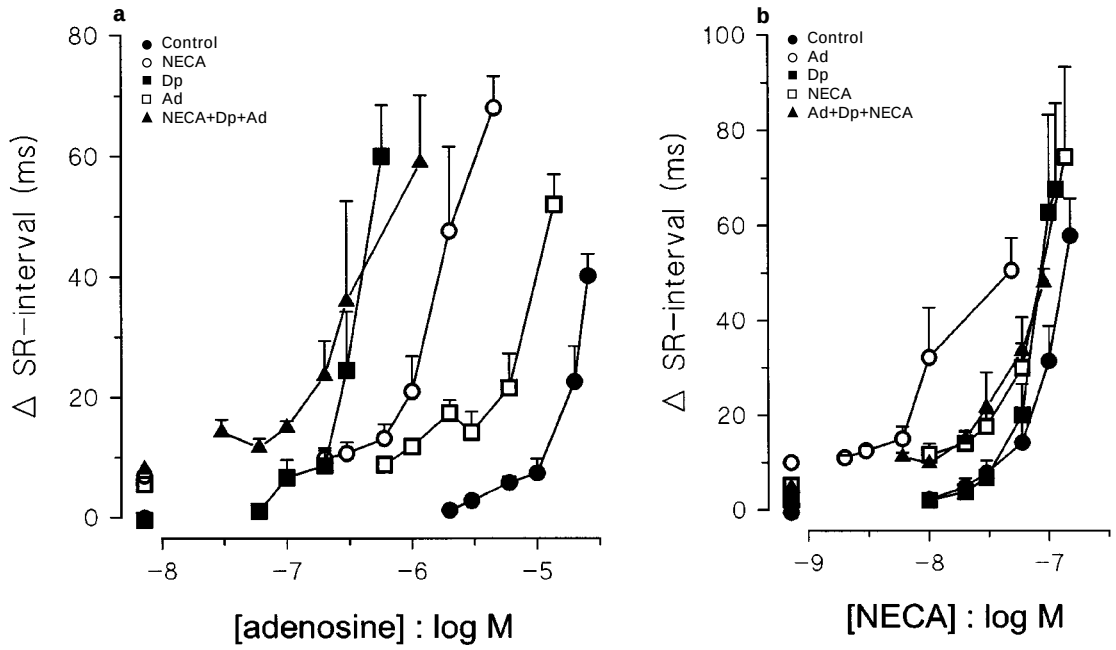

Figure 6 (a) Adenosine concentration-effect curve data obtained in the AV node assay in the absence (control) and presence of 60 nM NECA, 1 μM dipyridamole (Dp), 6 μM adenosine (Ad) and 60 nM NECA combined with 1 μM dipyridamole and 0.1 μM adenosine. (b) NECA concentration-effect curve data obtained in the AV node assay in the absence (control) and presence of 6 μM adenosine, 1 μM dipyridamole, 60 nM NECA and 0.1 μM adenosine combined with 1 μM dipyridamole and 60 nM NECA. The ten treatment groups were allocated to preparations according to a randomized block experimental design. Values represent mean of 5/6 preparations; vertical lines show s.e.mean. The results expressed in terms of $p[A]_{50}$ values are given in Table 1.

there was no significant displacement (log dose-ratio $=0.07\pm0.12$), indicating that there was no evidence of auto-potentiation. The mutuality of the NECA-adenosine interaction is shown in Figure 6b. The adenosine concentration-effect curve was displaced significantly to the left in the presence of 60 nM NECA (log dose-ratio $=0.84\pm0.20$). Judged by the $[A]_{50}$ values, a log dose-ratio value of 0.34 ± 0.14 was estimated, there was no evidence of adenosine auto-potentiation from the adenosine(6 μM)-adenosine interaction (see Discussion).

Are the assays strictly comparable?

Overall, the results of the study indicate that at the AV node, but not apparently at the SA node, adenosine can act at an intracellular site to potentiate the effects of adenosine A_1-receptor activation. With the model described below, this potentiation could explain why adenosine, in the absence of adenosine transport blockade, is more potent on the AV node than the SA node and why dipyridamole is more potent on the SA node. These conclusions of the study are based on the assumption that the data obtained on the two assays can be compared reliably. We were concerned about two major differences between the assays used to study the action of adenosine on the two nodes. First, AV node conduction was measured in a perfused assay system and SA node rate was measured in atria immersed in organ baths. Therefore, the endothelial cells, a major site of adenosine transport, and muscle cells were in parallel as far as diffusion of adenosine is concerned on the SA node and in series in the AV node. Second, the basal activity of the SA node was increased by administration of histamine to improve the assay signal-to-noise ratio. To test whether these two factors influenced the conclusions of the study, an additional experiment was performed on isolated, perfused, hearts while measuring rate rather than conduction time, in the absence of histamine. Adenosine E/[A] curves were obtained in the absence and presence of the saturating concentration of dipyridamole (3 μM). The adenosine $p[A]_{50}$ values (control 3.81 ± 0.22, 3 μM dipyridamole 5.92 ± 0.09; $n=5$) were not significantly different from those obtained on the guinea-pig isolated, right atrium assay (see Table 1), which indicates that differences in assay conditions were not contributing to the differences in the activity of adenosine between the nodes.

An explanatory model was developed to account for the data described above using existing pharmacological concepts of ligand action in isolated tissue bioassays.

Development of an explanatory model to account for the actions of adenosine on the AV node

First, model descriptions were sought for the following features of the experimental data. The concentration of adenosine, but not NECA, was apparently lowered in the receptor compartment due to the activity of a saturable uptake process which was competitively blocked by dipyridamole. Second, the pK_B or pA_2 values obtained for antagonists and an agonist potency order analysis (Meester *et al*., 1998) indicated that the agonists, adenosine and NECA, act at adenosine A_1-receptors which are located extracellularly. Third, adenosine and NECA potentiated the action of each other but only in the absence of uptake blockade so that the second action of adenosine is intracellular. The elements of the model are shown schematically in Figure 7a.

Agonist uptake A mathematical model to predict the effects of saturable agonist removal from the receptor compartment was first described by Waud (1969). In the model, agonist, A, is imagined to diffuse into the receptor compartment (governed by the diffusion constant, k_t) from where it is removed by a

saturable uptake process. The rate of diffusion A into the receptor compartment (D_{in}) is given by the following equation:

$$D_{in} = k_t \cdot ([A]_0 - [A]_i) \quad (2)$$

where $[A]_0$ = the concentration of A in the perfusion fluid and $[A]_i$ = the concentration of A in the receptor compartment. The rate of removal of A from the receptor compartment (J) is assumed to be governed by Michaelis-Menten kinetics and is given by:

$$J = \frac{J_{max} \cdot [A]_i}{K_M + [A]_i} \quad (3)$$

where J_{max} = the maximum rate of removal and K_M = the Michaelis-Menten rate constant for removal. At steady state, the rate of entry equals the rate of removal. Accordingly, by equating (2) and (3) and re-arranging, $[A]_i$ can be obtained as the positive root of the following quadratic function of [A]:

$$[A]_i = \frac{-b \pm \sqrt{(b^2 - 4ac)}}{2a} \quad (4)$$

where $a = 1$, $b = (K_M - [A]_0 + J_{max}/k_t)$ and $c = -([A]_0 . K_M)$. The effects of a competitive inhibitor of the uptake process, such as dipyridamole, can be examined by multiplying the parameter K_M by the factor $(1 + [I]/K_i)$, where [I] = the concentration of inhibitor and K_i = the equilibrium dissociation constant for the inhibitor-uptake site complex.

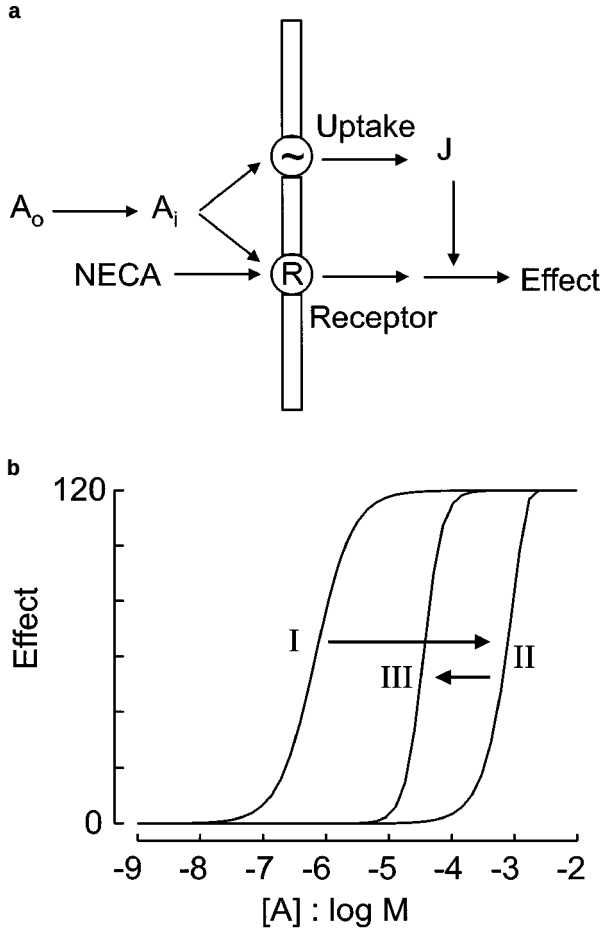

Figure 7 (a) Schematic diagram of the model developed to account for the potentiating interaction between NECA and adenosine in the AV node assay. (b) Simulations of the explanatory model showing adenosine curves obtained with and without adenosine uptake blockade by dipyridamole in the absence and presence of intracellular potentiation. The location of the adenosine curve is governed by the net effect of the rightward shift due to uptake decreasing the adenosine concentration and the leftward shift due to the potentiation produced as a consequence of the uptake. The following model parameter values were used (see text for details of the model): (I) control curve (i.e. no uptake and no potentiation. This condition was simulated in the model by setting K_M at a very high value, 1 M, and $z = 0$ mol^{-1} min). (II) uptake active but no potentiation allowed ($J_{max} = 1.5$ mmol min^{-1}, $K_M = 1$ μmol, $z = 0$ mol^{-1} min). (III) uptake and potentiation active ($J_{max} = 1.5$ mmol min^{-1}, $K_M = 1$ μM, $z = 10^6$ mol^{-1} min). The Hill equation (6) parameters were fixed as follows: $\alpha = 120$ ms; $n_H = 1.5$; $[A]_{50} = 0.6$ μM.

A_1-receptor-mediated agonism The agonist concentration-effect curves obtained in the AV node preparation did not have a defined upper asymptote due to the abrupt onset of 2nd or 3rd degree AV block. However, by assuming that the curves were truncated sigmoids, the following form of the Hill equation which gives pharmacological effect (E) in terms of the receptor compartment concentration of A ($[A]_i$) was used:

$$E = \frac{\alpha \cdot [A]_i^{n_H}}{[A]_{50}^{n_H} + [A]_i^{n_H}} \quad (5)$$

where α = the upper asymptote, $[A]_{50} = [A]_i$ required for 0.5α and n_H = the midpoint slope parameter. The choice of this equation allowed the use of established methods of expressing the potentiating interaction (see below) and the competition between the agonists for the A_1-receptor. Both adenosine (A) and NECA (N) produced the same maximum effect and were assumed to be high efficacy agonists. Therefore, the maximum response (α) and the slope of the curves (n_H) could be assumed to be identical and, empirically, by analogy to the Gaddum-Schild equation, the competitive interaction at the receptor could be expressed as follows:

$$E = \frac{\alpha \cdot [A]_i^{n_H}}{([A]_{50}(1 + [N]/[N]_{50}))^{n_H} + [A]_i^{n_H}} + \frac{\alpha \cdot [N]^{n_H}}{([N]_{50}(1 + [A]_i/[A]_{50}))^{n_H} + [N]^{n_H}} \quad (6)$$

where $[N]_{50}$ and $[A]_{50}$ are the midpoint location parameters of the NECA and adenosine curves, respectively.

Potentiation by adenosine in the absence of uptake blockade The potentiating interaction between adenosine and NECA was manifested as a parallel leftward shift of the agonist concentration-effect curves. In the equation (6) used to describe the A_1-receptor mediated agonist concentration-effect curves, the only parameters which govern the location of the curves are $[A]_{50}$ and $[N]_{50}$. Therefore, in the first instance, the additional potentiating action of adenosine was expressed as follows:

$$[A]_{50}* = [A]_{50}/(1 + S) \quad (7)$$

$$[N]_{50}* = [N]_{50}/(1 + S) \quad (8)$$

so that the $[A]_{50}$ values are decreased to $[A]_{50}$* values by the second intracellular action of adenosine which is mediated by the stimulus S. In the first instance, S was assumed to be linearly related to the rate of adenonsine entry into the cell (J in Equation 3), so that, the stimulus is a rectangular hyperbolic function of $[A]_i$ as follows:

$$S = z.J = z. \frac{J_{max} \cdot [A]_i}{K_M + [A]_i} \quad (9)$$

where z is a proportionality constant which governs the relationship between the rate of uptake and the production of the intracellular stimulus. The product of z and J_{max} determines

the maximum leftward shift due to the intracellular action of adenosine which can be obtained in the system (e.g. when $J_{max} = 10^{-3}$ mol min^{-1} and $z = 10^6$ mol^{-1} min then log dose-ratio = -3).

Behaviour of the model The overall model is given by the component equations which describe the agonist uptake (4), the A_1-receptor interaction (6), the intracellular potentiation (7),(8) and the production of the potentiating stimulus by the inward flux of adenosine (9). In practice, due to the inherent complexity of the system and the interdependence of the parameters and variables between these equations, a numerical solution can only be obtained by solving in the following order, (4), (9), (7), (8) and (6). In brief, the behaviour of the model can be summarized as shown in Figure 7b. The location of the adenosine concentration-effect curve is governed by the net effect of the rightward shift due to the uptake decreasing $[A]_i$ and the leftward shift due to the potentiation produced as the uptake increases the amount of intracellular adenosine. Similarly, the interaction between NECA and adenosine involves a small degree of rightward shift due to competition for the A_1-receptor and leftward shift due to the intracellular potentiating action of adenosine.

Application of the model First, the experimental data representing the effects of NECA in the absence and presence of adenosine in the guinea-pig SA and AV nodes (Figure 4) were simulated using the model (Figure 8a and b). Second, the model was applied simultaneously to the data from the randomized treatment experiment (Table 1 and Figure 6). For clarity of display, these model simulations are grouped in separate figures as follows: (a) adenosine, adenosine plus NECA and adenosine plus adenosine (Figure 9a), (b) NECA, NECA plus adenosine and NECA plus NECA (Figure 9b) and (c) adenosine and adenosine plus NECA in the absence and presence of uptake blockade by dipyridamole (Figure 9c). Finally, an attempt was made to simulate the data obtained in the experiment (Figure 5) which investigated the potentiation of NECA by 6, 10 and 15 μM adenosine (Figure 9d).

For each experiment, the values of the parameters $[A]_{50}$ and $[N]_{50}$ in the model were set to provide a good simulation of the control adenosine (plus dipyridamole) and NECA curves, respectively. In practice, these model values were $\sim$0.4 log units higher than the experimentally-defined $[A]_{50}$ values due to the truncation of the experimental E/[A] curves. For the same reason, the values of α for the model logistic function (equation (6)) were set at higher values than the experimentally-determined maximum responses (see Discussion). To simulate the effect of adenosine pre-incubation on the adenosine E/[A] curve, the value of [N] was set at the pre-incubation concentration of adenosine and $[N]_{50}$ to the value of the $[A]_{50}$

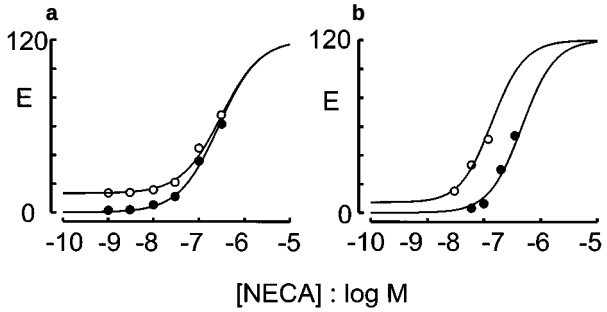

Figure 8 Experimental data showing the (a) negative chronotropic actions of NECA in the guinea-pig SA node in the absence (solid circles) and presence of 60 μM adenosine (open circles) and (b) negative dromotropic actions of NECA in the guinea-pig AV node in the absence and presence of 10 μM adenosine (from Figure 4). Superimposed on the data points are curves simulated using the explanatory model with the following parameter values (see text for details of the model): (a) $[N]_{50} = 0.27$ μM, $\alpha = 300$ beats min^{-1}, $n_H = 1$, $[A]_{50} = 0.65$ μM, $J_{max} = 0.8$ mmol min^{-1}, $K_M = 1$ μM, $z = 0$ mol^{-1} min, [A] = 0 and 60 μM. (b) $[N]_{50} = 0.47$ μM; $\alpha = 120$ ms; $n_H = 1.5$, $[A]_{50} = 0.85$ μM; $J_{max} = 0.3$ mmol min^{-1}, $K_M = 1$ μM, $z = 3.10^5$ mol^{-1} min, [A] = 0 (●) and 0.1 μM (○).

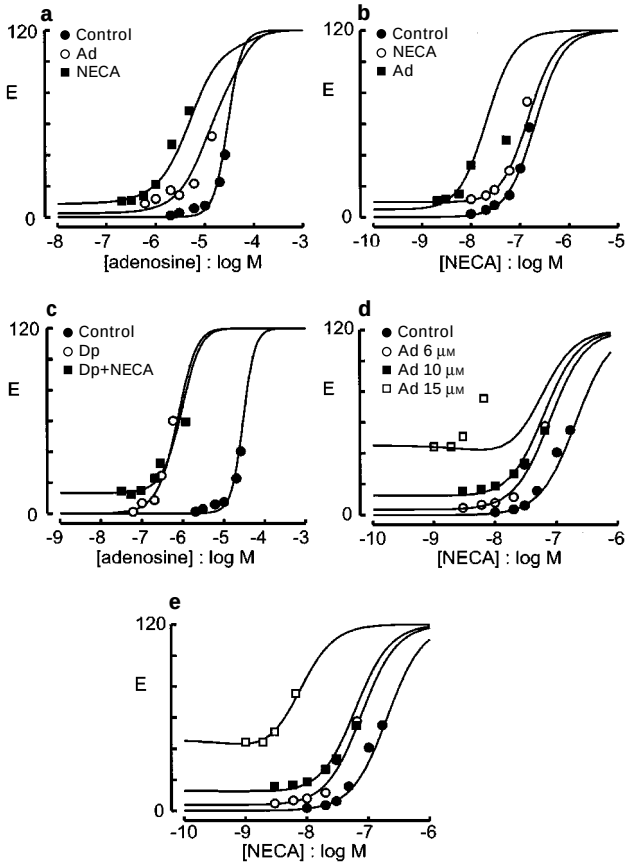

Figure 9 Experimental data showing the negative dromotropic actions in the guinea-pig AV node of (a) adenosine in the absence (control) and presence of 6 μM adenosine (Ad) and 6 nM NECA, (b) NECA in the absence (control) and presence of 60 nM NECA and 6 μM adenosine, (c) adenosine in the absence (control) and presence of 1 μM of the adenosine uptake inhibitor dipyridamole (Dp; assumed to saturate the uptake process, therefore for the model simulation the value of K_M was set at 1 M) and 1 μM dipyridamole and 60 nM NECA and (d) NECA in the absence (control) and presence of 6 μM, 10 μM and 15 μM adenosine. Superimposed on the data points are curves simulated using the explanatory model with the following parameter values (see text for details of the model): (a) $[A]_{50} = 0.6$ μM, $\alpha = 120$ ms, $n_H = 1.5$, $J_{max} = 1.5$ mmol min^{-1}, $K_M = 1$ μM, $z = 10^6$ mol^{-1} min, $[N]_{50}$ (=$[A]_{50}$ value for adenosine) = 0.6 μM (○) and 0.2 μM (■), [N] = 0 (●), 4.5 μM (i.e. the pre-incubation concentration of adenosine) (○) and 36 nM (■). (b) $[N]_{50} = 0.2$ μM; $\alpha = 120$ ms; $n_H = 1.5$, $J_{max} = 1.5$ mmol min^{-1}, $K_M = 1$ μM, $z = 10^6$ mol^{-1} min, $[A]_{50} = 0.6$ μM (○) and 0.2 μM (■), [A] = 0 (●), 40 nM (○) and 10 μM (■). (c) $[A]_{50} = 0.6$ μM, $\alpha = 120$ ms, n_H-1.5, $J_{max} = 1.5$ mmol min^{-1}, $z = 10^6$ mol^{-1} min, $[N]_{50} = 0.2$ μM, $K_M = 1$ μM (●), 1 M (○) and 1 M (■), [N] = 0 (●), 0 (○) and 50 nM (■). (d) $[N]_{50} = 0.2$ μM, $\alpha = 120$ ms, $n_H = 1.5$, $J_{max} = 0.3$ mmol min^{-1}, $K_M = 1$ μM, $z = 0$ (●), 3×10^5 (○), 3×10^5 (■) and 3×10^5 (□) mol^{-1} min, $[A]_{50} = 0.6$ μM, [A] = 0 (●), 6 (○), 10 (■) and 18 (□) μM. (e) A repeat stimulation of (d) in which the value of z was increased from 3×10^5 to 3×10^6 mol^{-1} min and J_{max} from 0.3 to 1.7 mmol min^{-1} for the NECA curve obtained in the presence of the highest concentration of adenosine (open squares; see text for details). All other parameter values were unchanged.

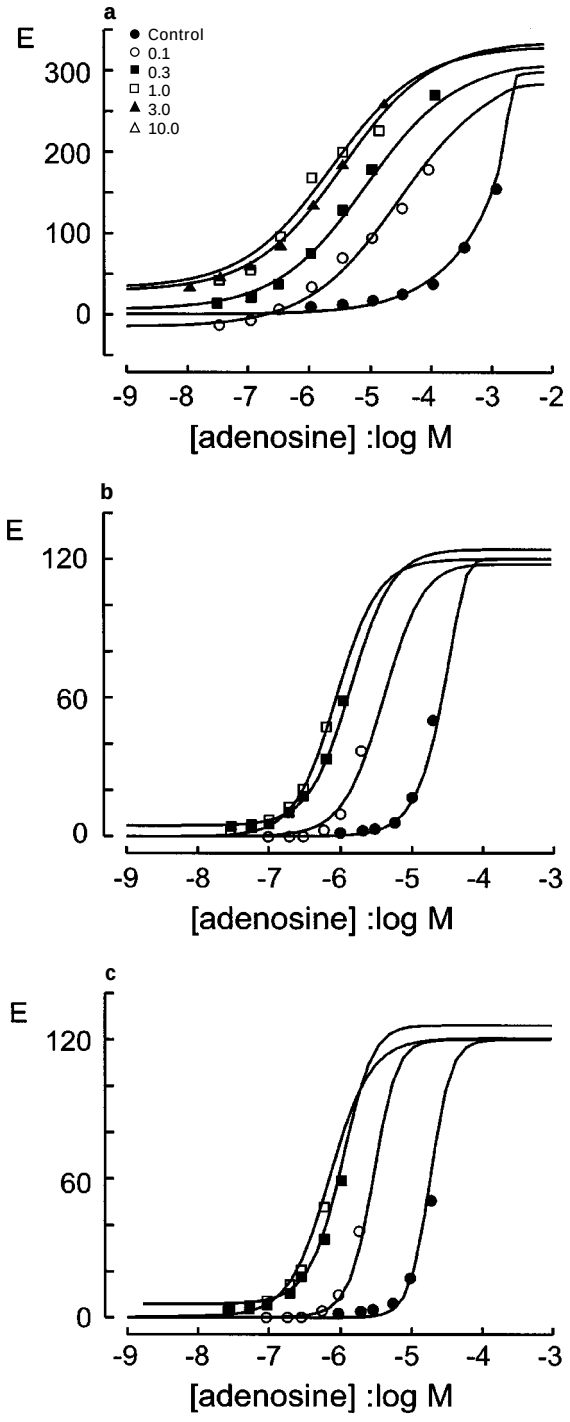

Figure 10 Adenosine concentration-effect curve data obtained in the SA node (a) and AV node assays (b and c) in the absence (control) and presence of 0.1, 0.3, 1, 3 and 10 μM dipyridamole (from Figure 2). Superimposed on the data points are curves simulated using the explanatory model with the following parameter values (see text for details of the model): (a) simulation of the SA node data using the model with no intracellular potentiation (i.e. $z_m = 0$ mol^{-1} min). $[A]_{50} = 1$ μM, $\alpha = 300$ beats min^{-1}, $n_H = 0.6$, $J_{max} = 2$ mmol min^{-1}, $K_M = 1$ (●), 80 (○), 280 (■), 800 (□), 1500 (▲) μM. The small effect of dipyridamole on basal rate was assumed to be due to an independent action which was modelled by simply adding a basal change in rate as follows: 0 (●), −16.4 (○), 5.9 (■), 33.6 (□), 29.2 (▲) beats min^{-1}. (b) Simulation of the AV node data using the model with no intracellular potentiation (i.e. $z = 0$ mol^{-1} min). $[A]_{50} = 0.6$ μM, $\alpha = 120$ ms, $n_H = 1.5$, $J_{max} = 0.07$ mmol min^{-1}, $K_M = 1$ (●), 12 (○), 52 (■), 150 (□) μM. The small effect of dipyridamole on basal rate was assumed to be due to an independent action which was modelled by simply adding a basal change in rate as follows: 0 (●), −1.2 (○), 5.5 (■), 1 (□) ms. (c) Simulation of the AV node data using the model with intracellular potentiation (i.e. $z = 10^6$ mol^{-1} min). $[A]_{50} = 0.6$ μM, $\alpha = 120$ ms, $n_H = 1.5$, $J_{max} = 0.6$ mmol min^{-1}, $K_M = 1$ (●), 36 (○), 250 (■), 800 (□) μM. The small effect of dipyridamole on basal rate was assumed to be due to an independent action which was modelled by simply adding a basal change in rate as follows: 0 (●), −1.2 (○), 5.5 (■), 1 (□) ms.

for the adenosine curve (Figure 9a). The value of the adenosine uptake parameter, K_M, ws fixed at 1 μM for all experiments whereas the values of J_{max} and z were adjusted to obtain the correct balance between the extent of uptake and the degree of potentiation. In practice, the values of J_{max} and z were allowed to vary slightly between experiments to account for the small degree of inter-experimental variation (see legends to Figures 8 and 9). Once these parameter values had been selected, all of data from the randomized treatment experiment were simulated concurrently.

The model provided a good description of the experimental data representing the effects of NECA in the absence and presence of adenosine in the guinea-pig SA and AV nodes (Figures 8a and b). Similarly, a good simulation was obtained of the randomized block experimental data, although it was found necessary to modify the model concentration of pre-incubated NECA and adenosine to account for the apparent discrepancy between the responses obtained during pre-incubation and the corresponding response levels in the control concentration-effect curves. When the model was applied to the experiment which investigated the concentration-dependent nature of the potentiation of NECA by adenosine (Figure 9d), a good fit was obtained for all data except the curve obtained in the presence of the highest concentration of adenosine (15 μM). Inspection of this stimulation indicated that the experimental curve was shifted further to the left than the simulated curve as though a greater degree of potentiation had occurred. Accordingly, by removing the constraint imposed by the first and simplest assumption of a linear function between the amount of intracellular adenosine ($[A]_i$) and the degree of potentiation (equations 7 and 8), it was possible to obtain a good simulation. In practice, this was achieved by allowing the value of z to vary for the highest concentration of adenosine (see legend of Figure 9d).

We also investigated whether the model could account for the observed differences in the potency of adenosine, in the absence of uptake blockade, and in the apparent pK_i estimates for dipyridamole between the guinea-pig SA and AV nodes. First, the data obtained in the experiment which investigated the effects of adenosine in the absence and presence of several dipyridamole concentrations in the guinea-pig SA node was simulated (Figure 10a), using model parameter values set to preclude any intracellular potentiating interaction. Second, the model was applied to the experimental data representing the same experiment in the guinea-pig AV node. Two simulations of the AV node data were made; both without (Figure 10b) and with (Figure 10c) intracellular potentiation of the extracellular receptor responses. In all three sets of simulations, the value of the adenosine $[A]_{50}$ parameter in the model was fixed to the experimentally-determined midpoint location of the most leftward shifted adenosine curve. For the simulations of the SA node data and the first simulation of the AV node results, S_{2m} was fixed at zero, since potentiation was not allowed to occur. The control value of the adenosine uptake parameter, K_M, was fixed at 1 μM, whereas J_{max} was obtained by estimating the best fit of the adenosine control curve (see legends to Figures 10a and b). When simulating the

AV node data set with potentiation, the control value of K_M was again fixed at 1 μM, and the value of S_{2m} and J_{max} were adjusted in order to find the correct balance between the extent of uptake and the degree of potentiation, as judged by the location of the adenosine control curve (see legend to Figure 10c). For all three simulations, the values of K_M for each adenosine curve obtained in the presence of dipyridamole were set to obtain the best description of data without prejudice to a value of pK_i for dipyridamole. The next step was to determine if the occurrence of adenosine auto-potentiation could account for the differences in the apparent pK_i values of 8.87 in the SA node, and 8.15 in the AV node in the absence of potentiation. However, the equivalent pK_i value for the AV node when the potentiating mechanism was operating was 8.79. Therefore, the model can explain the apparent difference in the potency of dipyridamole which indicates that the nucleoside transporters in the two assays are not different.

Discussion

Previously, we found that the adenosine receptors in guinea-pig SA and AV node assays were indistinguishable as judged by antagonist affinity estimates and agonist potency values (Meester *et al*., 1998). Moreover, the agonist potency values obtained on the two assays lay along the line of identity which indicated that the receptor-effector coupling was identical between the assays. The agonists were selected for receptor classification study on the basis that they were not significantly taken up by the adenosine transporter. In this study, in the absence of transport inhibition, we found that adenosine in the AV node was significantly more potent than in the SA node, although when the transporter was blocked by dipyridamole the difference disappeared so that in the presence of dipyridamole the adenosine potency data from the two assays also lay on the line of identity.

When considered in isolation, the comparison of the $p[A]_{50}$ values obtained on the two assays, in the absence and presence of the concentrations of dipyridamole which appeared to saturate the transporter, indicate that the functional capacity of the uptake (X_{max} in Kenakin's method, equation 1) was greater in the SA node assay than in the AV node assay. According to the model of agonist uptake (Waud, 1969 and equation 4), the capacity of the uptake process is governed by the ratio of the maximum rate of uptake (J_{max}) and the rate of diffusion (k_t). Tissue-dependent differences in one or both of these parameters would seem reasonable. However, the difference in apparent capacity of the adenosine transport between the assays was accompanied by a significant difference in the apparent affinity of the transport inhibitor, dipyridamole, as estimated by applying Kenakin's method (1981). Thus, dipyridamole was less effective in the AV node than in the SA node although in both assays it behaved as a simple competitive inhibitor of uptake. In the model, pK_i values are expected to be tissue-independent and so differences suggest transporter heterogeneity. These differences are unlikely to be a consequence of variation in X_{max} values as in Kenakin's analysis (1981) pK_i and X_{max} parameters are relatively independent.

Kenakin's method (1981) makes several assumptions about the experimental system which, if invalid, could lead to erroneous estimates of dipyridamole pK_i values. The method assumes that the agonist concentration in the receptor compartment is negligible compared to the equilibrium dissociation constant for the agonist of the uptake site, so that the uptake is operating under pseudo-first order conditions. This appears to be the case in both assays as the $p[A]_{50}$ values ($\sim$6.4) for adenosine, in the presence of concentrations of dipyridamole which evidently saturated the uptake process, were over 2.6 orders of magnitude greater than the pK_M value of 3.8 estimated for adenosine in guinea-pig cardiac myocytes by Clanachan *et al*. (1987). On this basis Kenakin's method is applicable to both assays.

However, Kenakin's method also assumes that both the uptake inhibitor and the agonist only express their primary pharmacological action in the assay. Thus, one alternative to adenosine transport heterogeneity as an explanation for the different pK_i values might be that dipyridamole expressed additional actions which confounded the analysis. Indeed, dipyridamole is recognized to express other actions such as phosphodiesterase inhibition (Kukovetz & Poch, 1970). Although not significant as tested, there did seem to be a trend towards a concentration-dependent increase in basal activity in both assays (Figure 2c), which was not consistent with the expected behaviour of a competitive uptake inhibitor unless there was a basal release of adenosine in the assays. Previously (Meester *et al*., 1998), we found that administration of competitive adenosine A_1-receptor antagonists had no inhibitory effect on basal activity in either assay, which indicates that if there was any basal release of adenosine then only sub-threshold concentrations were achieved in the receptor compartment. In addition, there were two features in the data which indicated that the basal effects of dipyridamole were independent of its action as an uptake blocker. First, the two lowest concentrations of dipyridamole (0.1 and 0.3 μM; Figures 2a and b) produced near-maximal leftward shift but had no effect on basal activity in either assay. Second, the effects of dipyridamole on basal activity continued to increase at concentrations which produced no further leftward shift of the adenosine concentration-effect curves. Overall, therefore, the effects of dipyridamole on basal assay activity did not appear to be confounding the analysis. However, this did not rule out the possibility that the analysis was invalidated by an action of dipyridamole which might only be seen during stimulation of the preparations. This possibility was rejected by studying the effect of dipyridamole on NECA E/[A] curves on the basis that this would expose other actions of dipyridamole which could affect the activity of adenosine but were independent of its transporter blocking action. The concentrations of dipyridamole which apparently saturated the transport of adenosine had no significant effect on the NECA concentration-effect curves in either assay.

Multiple adenosine uptake sites have been identified, only one of which is sensitive to dipyridamole (e.g. Thorn & Jarvis, 1996). However, the model that has been developed to account for the data only includes a single, dipyridamole-sensitive, adenosine uptake process. This simplification seemed justified according to the following argument. Dipyridamole produced a parallel leftward shift of the adenosine E/[A] curve in both assays (Figure 2a and b). We make the usual null-method assumptions for a one-receptor-effector system, that equal effects are produced by equal agonist-receptor occupancy. Therefore, the concentration of adenosine within the receptor compartment, in the absence and presence of dipyridamole, can also be assumed to be equal for equal effects. This means that in the absence and presence of dipyridamole, adenosine would gain the same access to any other sites of action from within the receptor compartment. If access to these sites was required for the potentiation, then it should still have been seen in the presence of dipyridamole. In the event it was not and, so, we concluded the only significant access to the potentiating site of action was via the dipyridamole-sensitive uptake.

NECA was also used to test whether adenosine could express an action other than A_1-receptor mediated agonism. The interaction experiments (Figure 6) indicated that adenosine potentiated the action of NECA in the AV node but not in the SA node. The subsequent experiments revealed that the potentiation in the AV node was concentration-dependent and reciprocal to the extent that pre-incubation with NECA also potentiated adenosine effects. As the potentiation disappeared in the presence of uptake blockade, the potentiating action of adenosine was concluded to be due to an intracellular site of action accessed via the transporter. It seems unlikely that NECA potentiated adenosine as a consequence of adenosine uptake block for two main reasons. First, NECA did not potentiate adenosine in the SA node assay, although there was a clear experimental 'window' to exhibit such an effect as judged by the potentiation observed with dipyridamole. Second, $\sim$1 log unit of potentiation of the adenosine E/[A] curve was observed in the presence of 60 nM NECA in the AV node assay (Figure 6a). If this effect was due to NECA behaving as a competitive inhibitor of the uptake then the K_i for NECA would have to be as low as $\sim$6 nM. However, NECA has been shown to interact at the uptake site with an apparent affinity of >100 μM (Clanachan *et al*., 1987).

The explanatory model was developed to see whether it was possible to account for the experimental data using existing pharmacological concepts of ligand action in isolated tissue bioassays. One of the first problems to be addressed was how to describe the agonist concentration-effect curves. The comparison of agonist potency values was potentially invalidated by the inability to define fully the chronotropic and dromotropic responses due to the abrupt onset of SA node arrest and AV node conduction block. Locating the concentration-effect curves by the concentration required for half-maximal effect ($p[A]_{50}$) does not have the same meaning as a $p[A]_{50}$ value calculated for a full sigmoid function because the upper asymptote was not defined. However, in practice, because of the consistent curve shape, both within and between assays and irrespective of any experimental treatments, the $p[A]_{50}$ values were measured at similar effect levels so that the comparison seems valid. Therefore, for simplicity, it seemed reasonable to consider the concentration-effect curves as truncated sigmoids and a standard logistic function was used to describe the data (equation 5). This raised the problem of selecting values for the model upper asymptote parameters. For the purpose of simulating the SA node data, a value of 300 beats min^{-1} was selected as this represented the maximum theoretical change in SA node rate which could be achieved by a negative chronotropic agent in view of the average basal rate in the assay which was $\sim$300 beats min^{-1} elevated from unstimulated basal rate of $\sim$200 beats min^{-1} by the addition of histamine (see Methods). For the AV node data simulation the upper asymptote was fixed at an arbitrary conductance interval of 120 ms. This value was below the theoretical maximum conductance period (286 ms) which is governed by the interval between the electrical stimuli applied to the preparation.

The model provided a good description of the experimental data representing the effects of NECA obtained in the absence and presence of adenosine in the guinea-pig SA and AV nodes (Figure 8). Similarly, good fits were obtained for data from the randomized block experiment, which were simulated concurrently using almost identical parameter values (Figure 9). The only adaptation that was made in order to obtain optimal curve fits was a slight change in the model value of the concentration of the pre-incubated agonists (see legend to Figure 9). The need for this change could be explained by the steep slope of the adenosine and NECA curves in the guinea-pig AV node. When agonist curves are steep, a small change in agonist potency between experiments can produce a relatively large change in the response to fixed concentrations of agonist. Alternatively, the differences in response to single, pre-incubation doses could be due to time-related changes in the responsiveness of the tissue during the agonist pre-incubation period which was longer than the time allowed when the agonist responses were obtained by cumulative dosing.

When the model was applied to the experimental results representing the concentration-dependent potentiation of NECA by adenosine (Figure 9d), it provided a good description for all data except the NECA curve obtained after pre-incubation with the highest adenosine concentration used (15 μM). The model-simulated curve was found to lie to the right of the experimental curve, which indicates that the potentiation which had occurred was larger than predicted. Since the degree of potentiation is governed in the model by a linear function of the intracellular stimulus S (equations 7 and 8), this constraint was removed by allowing z to increase for the highest concentration of adenosine (see legend to Figure 9e). When this increase in z was combined with an increase in J_{max}, the corresponding simulation yielded a good fit. This indicates that, firstly, the relationship between potentiation and S may not be linear but rather an upward concave function, as expected if the interaction is positively co-operative, and secondly, that the rate of influx increases significantly at higher adenosine concentrations. Indeed, although the uptake of adenosine occurs mainly through carrier-mediated facilitated-diffusion systems, it has been demonstrated that at the higher concentrations simple diffusion through the cell membrane becomes more important (Roos & Pfleger, 1972).

One of the features of the model is that adenosine, in the absence of transport block, can potentiate itself. The finding that pre-incubation of the AV node assay with adenosine did not result in significant potentiation as judged by the $[A]_{50}$ values (log dose-ratio value of 0.34 ± 0.14) is explained by the fact that the control curve is already auto-potentiated. Thus, the effect of the relatively low concentration of pre-incubated adenosine is predicted to potentiate only the lower region of the adenosine E/[A] curve obtained at adenosine concentrations less than 6 μM. Inspection of the data in this region (Figure 6a) and the model simulation (Figure 9a) reveals this behaviour which contrasts with the effect of NECA pre-incubation on NECA E/[A] curves (Figure 6b) where no potentiation is predicted (Figure 9b). The auto-potentiation expressed by adenosine was also found to provide an explanation for the apparent underestimation of the affinity of dipyridamole for the adenosine transporter in the AV node (Figure 2). Thus, the potentiation produced by inhibiting the removal of adenosine from the receptor compartment was simultaneously offset by the decrease in potentiation produced by the intracellular adenosine. In practice, the adenosine-dipyridamole interaction data in the AV node was simulated by fixing the maximum degree of intracellular potentiation at the value used in the simulations of the other interaction experiments (i.e. $z = 10^6$ mol^{-1} min, Figure 10c). This degree of potentiation was sufficient to rectify the dipyridamole pK_i value to one which was indistinguishable from that obtained in the SA node. However, to get a good simulation of the data, it was necessary to set the maximum rate of adenosine transport (J_{max}) to a value which was still 3 fold higher than in the SA node. In fact, an equally good simulation of the data could be obtained by fixing the value of J_{max} between the assays and allowing the value of z to alter by 3 fold between experiments.

The model allowed us to test whether the previously unrecognized, tissue-dependent, potentiating action of adenosine could account for the differences in the apparent potency of dipyridamole and adenosine between the SA and AV node assays. The idea that adenosine is pharmacologically active at an intracellular site is not new. It was originally described as a binding site, the so-called P-site (Londos & Wolff, 1977), but Olsson & Pearson (1990) subsequently showed that it was coupled to inhibition of adenylate cyclase. The potentiation interaction which we have described is a pharmacological phenomenon and our analysis gives no clue as to what, if any, is its physiological significance.

This work was funded by the Wijnand M. Pon Foundation (Leusden, The Netherlands) and the Interuniversity Cardiology Institute of the Netherlands.

References

BLACK, J.W., GERSKOWITCH, V.P., LEFF, P. & SHANKLEY, N.P. (1985). Pharmacological analysis of β-adrenoceptor-mediated agonism in the guinea-pig, isolated, right atrium. *Br. J. Pharmacol.,* **84,** 779 – 785.

BLUM-KAELIN, D., ISLER, D., MOEGLEN, C., STROHM, G. & MEIER, M.K. (1991). Atypical β-adrenoceptors mediating thermogenesis in rat brown adipocytes. Consistency of binding and functional data using CGP 121777. In *Adrenoceptors: Structure, Mechanism, Function*. ed. Szabadi, E. & Bradshaw, C.W. Basel: Birkhauser Verlag.

CLANACHAN, A.S., HEATON, P. & PARKINSON, F.E. (1987). Drug interactions with nucleoside transport systems. In *Topics and Perspectives in Adenosine Research*. ed Gerlach E. & Becker, B.F. pp. 118 – 129. Berlin-Heidelberg: Springer-Verlag.

DOHRING, H.J. & DEHNERT, H. (1986). *The Isolated Perfused Heart According to Langendorff*. March, West-Germany: Biomesstechnik-Verlag.

DRURY, A.M. & SZENT-GYORGYI, A. (1929). The physiological activity of adenine compounds with especial reference to their action upon the mammalian heart. *J. Physiol.,* **68,** 213 – 237.

JENKINS, J.R. & BELARDINELLI, L. (1988). Atrioventricular nodal accommodation in isolated guinea pig hearts: Physiological significance and role of adenosine. *Circ. Res.,* **63,** 97 – 116.

KENAKIN, T.P. (1981). A pharmacological method to estimate the pK_I of competitive inhibitors of agonist uptake processes in isolated tissues. *Naunyn-Schmiedeberg's Arch. Pharmacol.,* **316,** 89 – 95.

KUKOVETZ, W.R. & POCH, G. (1970). Inhibition of cyclic-3′5′-nucleotide-phosphodiesterase as a possible mode of action of papaverine and similarly acting drugs. *Naunyn-Schmiedeberg's Arch. Pharmacol.,* **267,** 189 – 194.

LONDOS, C. & WOLFF, J. (1977). Two distinct adenosine-sensitive sites on adenylate cyclase. *Proc. Natl. Acad. Sci. U.S.A.,* **74,** 5482 – 5486.

MEESTER, B.J. PRENTICE, D.J., WELSH, N.J., SHANKLEY, N.P. & BLACK, J.W. (1993). Comparison of adenosine potentiation by dipyridamole in the atrioventricular and sinoatrial nodes and atrial muscle of the guinea pig. *Br. J. Pharmacol.,* **110,** 140P.

MEESTER, B.J., WELSH, N.J., SHANKLEY, N.P., MEIJLER, F.L. & BLACK, J.W. (1994a). Classification of adenosine A_1 receptors by agonist potency orders in the sinoatrial and atrioventricular nodes of the guinea-pig. *Br. J. Pharmacol.,* **112,** 580P.

MEESTER, B.J., WELSH, N.J., SHANKLEY, N.P., MEIJLER, F.L. & BLACK, J.W. (1994b). Potentiating interaction between adenosine and 5-N-ethylcarboxamidoadenosine in the guinea-pig atrioventricular node. *Br. J. Pharmacol.,* **112,** 582P.

MEESTER, B.J., SHANKLEY, N.P., WELSH, N.J., WOOD, J., MEIJLER, F.L. & BLACK, J.W. (1998). Comparative pharmacological analysis of adenosine receptors in the sinoatrial and atrioventricular nodes of the guinea-pig. *Br. J. Pharmacol.,* **124,** 685 – 692.

OLSSON, R.A. & PEARSON, J.D. (1990). Cardiovascular purinoceptors. *Physiol. Rev.,* **70,** 761 – 845.

RIBEIRO, J.A. & SEBASTIAO, A.M. (1986). Adenosine receptors and calcium: basis for proposing a third (A_3) adenosine receptor. *Prog. Neurobiol.,* **26,** 179 – 209.

ROOS, H. & PFLEGER, K. (1972). Kinetics of adenosine uptake by erythrocytes, and the influence of dipyridamole. *Mol. Pharmacol.,* **8,** 417 – 425.

THORN, J.A. & JARVIS, S.M. (1996). Adenosine transporters. *Gen. Pharmacol.,* **27,** 613 – 620.

WAULD, D.R. (1969). A quantitative model for the effect of a saturable uptake on the slope of the dose-response curve. *J. Pharmacol. Exp. Ther.,* **167,** 140 – 141.

(Received December 18, 1997
Revised February 13, 1998
Accepted March 16, 1998)